

RESEARCH

Open Access



Do wolframín, P-glycoprotein, and GRP78/BiP cooperate to alter the response of L1210 cells to endoplasmic reticulum stress or drug sensitivity?

Simona Kurekova^{1,2†}, Lucia Pavlikova^{1†}, Mario Seres^{1†}, Viera Bohacova¹, Jana Spaldova³, Albert Breier^{1,3*} and Zdena Sulova^{1*}

Abstract

In previous research, we revealed that murine leukemia cells L1210 with induced expression of P-glycoprotein (P-gp, a membrane drug transporter, product of the *Abcb1* gene) are better able to withstand endoplasmic reticulum (ER) stress (ERS) than their P-gp negative counterparts. This was associated with increased GRP78/BiP expression and modulation of the expression of several other proteins active in the cellular response to ERS (like CHOP, spliced XBP1, 50-kDa ATF6 protein fragment and others) in P-gp positive cells. Wolframín is an ER transmembrane protein, product of the *WFS1* gene whose mutations are associated with Wolfram syndrome. However, this protein is frequently overexpressed in cells undergoing ERS and its expression may accompany changes in the above ERS markers. Therefore, our aim in this work was to investigate wolframín expression in P-gp-negative and P-gp-positive murine leukemia L1210 cells in relation to ERS related proteins in normal or ERS condition. We induced ERS in cells either by blocking N-glycosylation in the ER with tunicamycin or by blocking ER Ca²⁺-ATPase activity with thapsigargin, as known ER stressors. The results of this paper demonstrated increased wolframín expression in P-gp positive cells compared to P-gp negative cells. Immunoprecipitation experiments revealed the formation of complexes between wolframín and ERS related proteins (PERK, ATF6 and GRP78/BiP), the amount of which varied depending on the presence of the above ER stressors.

Keywords Wolframín, P-glycoprotein, GRP78/BiP, PERK, ATF6, CHOP, XBP1, L1210 mice leukemia cells, Tunicamycin, Thapsigargin

[†]Simona Kurekova, Lucia Pavlikova and Mario Seres have contributed equally.

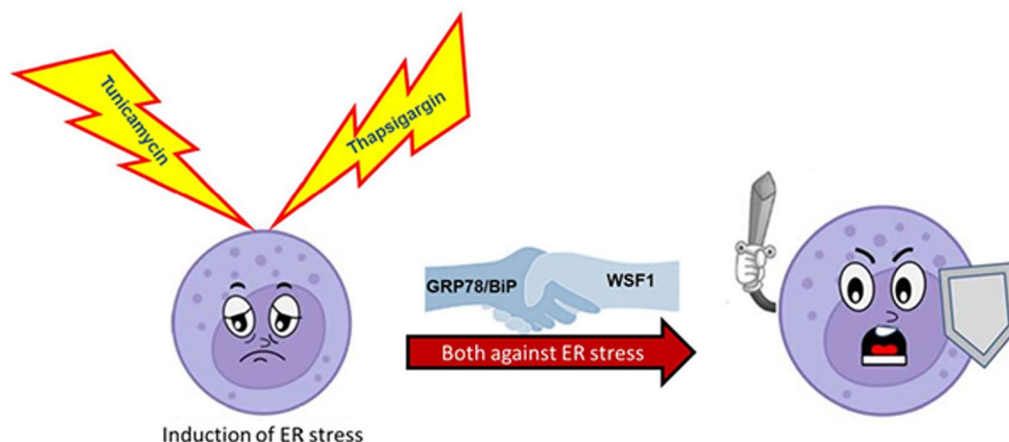
*Correspondence:

Albert Breier
albert.breier@stuba.sk
Zdena Sulova
zdena.sulova@savba.sk

Full list of author information is available at the end of the article



Graphical Abstract



Introduction

Multidrug resistance (MDR) of neoplastic cells, in which the cellular sensitivity to various drugs with different structures and mechanisms of action is significantly reduced, represents a serious obstacle for cancer chemotherapy (reviewed in [1]). There are several known and understood mechanisms of MDR development, among which the overexpression of membrane transporters from the ABC family, which are universal cellular detoxifiers within their broad substrate specificity, is very common (reviewed in [2]). In particular, P-glycoprotein (P-gp), the product of the *Abcb1* gene, which is the first ABC transporter discovered [3], is the most common, and targeted inhibition of its transport activity is thought to enhance chemotherapy-induced multidrug-resistant tumor cell death [4].

The endoplasmic reticulum (ER) is a cellular organelle that plays a key role in cellular homeostasis by ensuring important processes such as maintaining the intracellular Ca^{2+} ion concentration [5], controlling the initiation of N-glycosylation of nascent proteins with a key role for their proper folding [6], or participating in the cellular response to pro-oxidant stress [7]. An imbalance in these processes could lead to endoplasmic reticulum stress (ERS, reviewed in [8]). While the cytosol-oriented surface of the rough ER is the site of proteosynthesis, proper protein folding takes place in the lumen of the ER and involves the initial N-glycosylation of the newly formed protein [9]. This process involves the participation of the calcium dependent chaperones calnexin and calreticulin, which, in addition to helping in the proper processing of proteins, recognize defective and misfolded proteins and subject them to degradation by the proteasome in

the ER-associated protein degradation (ERAD reviewed in [10]). The dependence of both chaperones on the presence of Ca^{2+} in the ER connects the process of controlling intracellular calcium concentration and the process of proper protein folding. Therefore, thapsigargin (Thap, structure is given in Figure S1 in supplementary files), which primarily blocks the calcium pump in ER (product of *Serca* genes), eliminates the deposition of calcium within ER and thus makes the protein folding process impossible [11]. Another substance that interferes with the protein folding process is the N-glycosylation blocker tunicamycin (Tun structure is given in Figure S1 in supplementary files) [12]. Both mentioned substances cause accumulation of unfolded proteins within ER and subsequent ER stress. Due to the accumulation of immature misfolded proteins, the cell initiates a specific unfolded protein response (UPR). During the UPR, specific ERS receptors (such as activator transcription factor 6 ATF6 encoded by *Atf6* gene, pancreatic ER kinase PERK encoded by *Eif2ak3* gene, and serine/threonine protein kinase/endoribonuclease also known as inositol-requiring enzyme 1 IRE1 encoded by the *Ern1* gene) are activated. These receptors trigger mechanisms leading to a reduction in the amount of misfolded proteins, which enables cell survival [13, 14]. If ERS is so intensive or persistent that these receptors cannot suppress it, programmed cell death mechanisms are activated [15]. All three stress receptors are inactive on the ER in non-stress conditions as they are blocked by their endogenous protein inhibitor GRP78/BiP (78-kDa glucose-regulated protein known also as binding

immuno-globulin protein or heat shock 70 kDa protein 5, encoded by *Hspa5* gene), reviewed in [16].

Wolframin (WFS1 the product of the *WFS1* gene), mutations of which leads to Wolfram syndrome, is an integral protein of the ER [17]. WFS1 is a glycosylated protein, which was detected and proven by Western blotting of an untreated and deglycosylated sample by endoglycosidase H [18]. Replacement of Asn-663 and Asn-748 to be N-glycosylated with Asp by site-directed mutagenesis revealed variations in glycosylation and faster degradation of WFS1 under ERS induced with Tun [19]. There are suggestions that WFS1 could function as another ER calcium channel [20], or it is a regulator of the activity of known ER calcium-releasing channels [21]. Thus, WFS1 helps in ensuring the intracellular homeostasis of Ca^{2+} ions and has an effect on the folding of proteins in the ER [22]. If mutations of the *WFS1* gene lead to aberrations of its correct folding in the ER, ERS is induced, which is accompanied by disruption of the cell cycle and premature entry into apoptosis. Accordingly, WFS1 is thought to be a negative regulator in ERS development due to the UPR (reviewed in [23]).

Several lines of evidence have suggested that ERS-initiated processes may modulate the sensitivity of neoplastic cells to various drugs [16, 24–26]. Such a relationship may be closer because P-gp positive L1210 cells showed higher expression of GRP78/BiP (at both mRNA and protein levels) than their P-gp negative counterparts [27, 28]. Moreover, the increase in GRP78/BiP expression in P-gp-positive cells was accompanied by modulation of the expression of other ERS markers, such as stress induced proapoptotic protein CHOP (C/EBP homologous protein, encoded by *Ddit3* gene), spliced XBP1 (transcription factor X box protein 1 encoded by spliced transcript *sXbp1*), 50 kDa ATF6 protein fragment, etc. Connections between the expression of some ABC transporters (ABCB1, ABCC1–5 isoforms and ABCG2) and the ERS receptor PERK were also found [26].

Thus, there could be a link between the regulation of cellular response to ERS with the expression/function of both P-gp [27, 28] and WFS1 [22]. To verify such a possibility, we undertook to investigate whether there are differences in *Wfs1* gene expression (at the mRNA and protein level) between P-gp negative and P-gp positive variants of L1210 cells in response to ERS induced by Tun or Thap. Furthermore, by immunoprecipitation we detected the formation of complexes between WFS1 and ERS protein anchors (PERK, ATF6, and GRP78/BiP).

Materials and methods

Chemicals

Tun and Thap were supplied by the Merck group via MERCK spol. s.r.o. (Bratislava, Slovak Republic). Hoechst 34,580 was from Invitrogen via Thermo Fisher Scientific, (Bremen, Germany). Unless otherwise stated, all other chemicals were for laboratory use and were supplied by MERCK spol. s.r.o.

Cells and cultivation conditions

The drug-sensitive mouse lymphoblastic line L1210, which does not express P-gp (ACC-123), was obtained from the Leibniz-Institut DSMZ-Deutsche Sammlung von Mikroorganismen und Zellkulturen GmbH (Braunschweig, Germany) and is designated as variant S. The P-gp-positive drug-resistant variant of L1210 cells (designated as R) was prepared and maintained by selection of S cells with vincristine [29]. Some characteristics of the R variant compared to the S variant are shown in Table S1 (in Supplementary files). Cells were cultured in RPMI 1640 medium containing 8% fetal bovine serum, L-glutamine and 20 μ g/L gentamicin (all purchased from GIBCO, Langley, OK, USA) in a humidified atmosphere with 5% CO_2 in air at 37 °C. These L1210 cell variants (inoculum 10^6 cells) were passaged in 5 ml cultivation medium in Petri dishes for 24 h in

Table 1 Primers for qRT PCR

Gene	Forward primer	revers primer	bp
<i>Ddit3</i> ^a	5'-AGG TGA AAG GCA GGG ACT CA-3'	5'-CCA CCA CAC CTG AAA GCA GAA-3'	67
<i>sXbp1</i> ^a	5'-GTC CAT GGG AAG ATG TTC TGG-3'	5'-CTG AGT CCG AAT CAG GTG CAG-3'	59
<i>usXbp1</i> ^a	5'-GTC CAT GGG AAG ATG TTC TGG-3'	5'-CAG CAC TCA GAC TAT GTG CA-3'	76
<i>tXbp1</i> ^a	5'-GTC CAT GGG AAG ATG TTC TGG-3'	5'-TGG CCG GGT CTG CTG AGT CCG-3'	71
<i>Actb</i> ^b	5'-TCG CCA TGG ATG ACG ATA-3'	5'-CAC GAT GGA GGG GAA TAC AG-3'	110
<i>Atf6a</i> ^b	5'-GAG CCG CAC AGC TAC CTA AC-3'	5'-CCC ATA CTT CTG GTG GCA CT-3'	121
<i>Eif2ak3</i> ^b	5'-CTG CTG CTT CTG TTC CTG CT-3'	5'-CCC CTA AGC CAA ACA CTG TC-3'	106

^a primers adopted from [32]; ^b primers designed by program Primer 3 using the databases National Center for Biotechnology Information and Ensemble library; us—unspliced Xbp1; s—spliced Xbp1; t—primers did not recognize between spliced and unspliced version Xbp1

the presence of either Tun or Thap (both at 0.1 μ M) in culture conditions prior to analyses. As controls, cells were passaged in the same manner but in the absence of Tun or Thap.

Protocol used for RT-PCR and qRT-PCRs

Cells S and R after passage were harvested by centrifugation and 3×10^6 were used for total mRNA isolation. Total mRNA was isolated from variants of L1210 cells using TRI reagent (Molecular Research Center, Inc. Cincinnati, OH, USA) according to the manufacturer's instructions. Reverse transcription was performed using the RevertAid. H Minus First Strand cDNA Synthesis Kit (Thermo Fisher Scientific) according to the manufacturer's protocol.

The expression level of the *Wfs1* gene was determined using the obtained cDNA with following PCR procedure [30]. PCR was performed in a total volume of 25 μ L, which contained Taq Green MasterMix, DNase-free water, forward primer (5'-AAG GCT GCC CTG GTC ATG TA-3'), and reverse primer (5'- CCG TAC TCT CAC CGA CCT GC-3'), resulting in a 600 bp PCR product. As an internal standard, the gene for β -actin was used with forward primer (5'-TCG CCA TGG ATG ACG ATA-3') and reverse primer (5'-CAC GAT GGA GGG GAA TAC AG-3') gave 110 bp PCR product. After treating samples at 94 °C for 3 min to inactivate reverse transcriptase, samples were subjected to 30 cycles of 95 °C for 30 s followed by 57 °C for 30 s, depending on the primer used and incubation at 72 °C for 90 s and a final extension at 72 °C for 10 min. PCR products were separated in a 1.5% agarose gel (Lonza Group Ltd, Basel Switzerland) and visualized using GelRed™ nucleic acid gel stain (Thermo Fisher Scientific). Stained gels were imaged using an Amersham™ Imager 600 (GE Healthcare Bio-Science) and quantification of gel bands was processed by densitometry using Image Amersham™ software (GE Healthcare). Data were normalized to β -actin mRNA and expressed as mean \pm SD of three independent measurements. To prove the identity of the *Wfs1* PCR product, it was eluted from the gel and sent for sequencing at Eurofins Genomics Germany GmbH.

Quantitative levels of genes active in response to ERS (Table 1) were estimated using cDNA and respective primers (Table 1) by following qPCR protocol [31].

Samples were mixed with iTaq Universal SYBR Green Supermix (Bio-Rad Laboratories, Hercules, CA, USA) for qPCR. For the thermal cycle reactions, a CFX96 Real-Time System C1000 Touch Thermal Cycler (BioRad,

Laboratories, Hercules, CA, USA) was used with the following conditions: 95 °C for 10 min and then 39 cycles at 95 °C for 15 s and at 59 °C for 30 s. The relative amount for each transcript was calculated by a standard curve of cycle thresholds for cDNA samples and normalized to the amount of β -actin. The PCR was performed in triplicate for each sample, after which all experiments were repeated twice. The data were analyzed with Bio-Rad CFX96T software.

Western blotting

The protein levels were semiquantitatively determined by Western blotting. Cells were harvested and 10×10^6 were lysed with SoluLyse reagent containing a protease inhibitor cocktail (both from Sigma-Aldrich, St. Louis, MO, USA) and centrifuged at $12,000 \times g$ for 10 min. Protein lysates (30 μ g per lane) were separated by SDS-PAGE (according to Laemmli protocol described in [33]) on a Mini-Protean gel electrophoresis system (Bio-Rad, Philadelphia, PA, USA). Proteins were transferred by electroblotting (using Towbin protocol described in [34]) to a polyvinylidene fluoride membrane (GE Healthcare Europe GmbH, Vienna, Austria) and identified by using the following primary antibodies: rabbit polyclonal antibodies against WFS1 (26995-1-AP) were from Proteintech Group, Inc (Rosemont, IL, USA), β -Actine, (ab8227) were from Cell Signaling Technology, Inc (Beverly, MA, USA), mouse monoclonal antibodies against ATF6 (sc-166659) were from Santa Cruz Biotechnology, (Dallas, TX, USA) and tubulin (ab56676) were from Abcam (Boston, MA, USA). Goat anti-mouse and anti-rabbit secondary antibody linked with horseradish peroxidase were from Cell Signaling Technology, Inc. (Beverly, MA, USA). The proteins were visualized with an enhanced chemiluminescence detection system (GE Healthcare Europe GmbH, Vienna, Austria) using an Amersham Imager 600 (GE Healthcare). Broad range protein molecular mass markers (Thermo Fisher Scientific) were used as standards. The intensity of protein bands was quantified by densitometry by using Image Amersham image analysis software (GE Healthcare). All samples were analyzed in triplicate, and the intensity levels were normalized to β -actine or tubulin as a house-keeping protein. Significance was established using an unpaired Student's t-test.

Immunocytochemistry

The variants of L1210 cell (R and T) after passaging in the absence or presence of either Tun or Thap were harvested and were fixed with 3.7% paraformaldehyde in

PBS (phosphate buffered saline obtained from Thermo Fisher Scientific) for 10 min at room temperature. The cells were then permeabilized with 0.1% TritonX-100 for 15 min/4 °C and finally blocked for 1 h with 0.1% Tween20 containing 1% BSA (bovine serum albumin) in PBS incubated at room temperature. Then the specimens were 3× washed with 0.1% Tween20 in PBS 3 for 5 min and left to interact overnight with primary antibodies against WFS1 (1: 250, 26995-1-AP, Proteintech), SERCA2 (1: 100, MA3-910, Thermo Fisher Scientific), IPR32 (1:50, sc-398434, Santa Cruz Biotechnology) at 4 °C. The samples were washed 3× with PBS and incubated with Goat anti-Rabbit 550 (1: 1000, A32732, Invitrogen) and Goat anti-Mouse (1: 1000, A32723, Invitrogen) secondary antibodies. The specimens were finally washed 3 times in PBS and then incubated with Hoechst 34580 (1 µg/mL, Invitrogen) in PBS for 20 min at room temperature to visualize nuclei. Imaging was performed on a confocal microscope (Leica TCS SP8, Leica Microsystems, Germany) with an objective HC PL APO CS2 63×/1.4 NA OIL. We captured the images using LAS X software (Leica Microsystems, Germany). We used xy-scan mode with a scan frequency of 700 Hz. Picture analysis and fluorescence quantification from microscopic screen were processed using Fiji software according to Schindelin et al., [35].

Immunoprecipitation procedure

L1210 cell variants after passaging in the absence or presence of either Tun or Thap were harvested, and whole cell lysates were prepared from 10×10^6 cells. The lysates were used for immunoprecipitation according to the following protocol [36]. Proteins (160 µg, determined by Lowry assay [37]) were dissolved to a final volume of 300 µL using 50 mM Tris-HCl (pH 7.0) containing 5 µg antibodies against either the ATF6, PERK, GRP78/BiP or WFS1 (rabbit polyclonal anti-WFS1 antibody ab259362, anti-GRP78/BiP ab21685 was from Cell Signaling Technology, Inc; mouse monoclonal anti-PERK antibody sc-377400 was from Santa Cruz Biotechnology and anti-ATF6 antibody was same as described in Sect. "Western blotting"). After 2 h of incubation at 4 °C, 20 µL of protein A/G PLUS-agarose (Santa Cruz Biotechnology, Dallas, TX, USA) was added, and the mixture was incubated overnight at 4 °C. The agarose was then pelleted by centrifugation (10 min at 10,000 rpm) at 4 °C and washed twice with 50 mM Tris-HCl buffer. The agarose-bound proteins were solubilized directly in SDS-PAGE sample buffer, loaded onto a 10% gel, and electrophoretically separated. The proteins were then electroblotted onto a PVDF membrane, and the presence of WFS1 or GRP78/BiP in the immunoprecipitates were detected using the antibodies as described above. The intensity of all bands

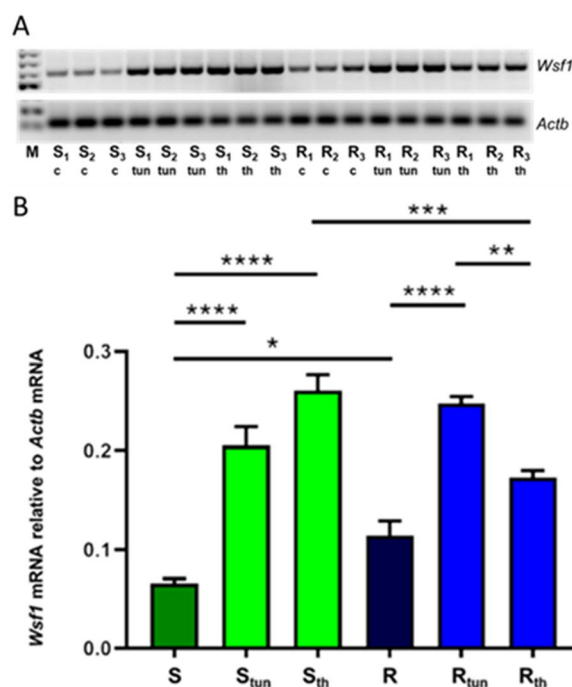


Fig. 1 Changes in relative gene expression of *Wfs1* in S and R cells in the absence (c) or presence of either Tun (tun, 0.1 µM) or Thap (th, 0.1 µM). Cells were passaged for 24 h and then harvested for isolation of total RNA and subsequent RT-PCR. **A** Electrophoretic visualization of the respective PCR products. The *Actb* gene (encoding β-actin) was used as an internal control. **B** The optical densities of the PCR bands were quantified and are summarized in bar graphs. Data are expressed as mean ± SD of three independent measurements. Statistical significance: Marked data differ on the level: * $p < 0.1$ marginally significant; ** $p < 0.02$ significant; *** $p < 0.01$ significant; **** $p < 0.001$ very significant

was compared with the control, taking into account that equal amounts of immunoprecipitating antibody (5 µg) and Protein A/G PLUS-agarose (20 µL) were added to the reaction. The homogeneity of the application of immunoprecipitates for Western blot detection is documented for the immunoprecipitate obtained with the rabbit anti-WFS1 antibody using the protein bands of the light and heavy subunits of rabbit IgG by the secondary goat anti-mouse antibody linked with horseradish peroxidase (Supplementary files Figure S2).

Protein deglycosylation by peptide:N-glycosidase F

After passaging, S cells were harvested and then 10×10^6 cell were added to sample deglycosylation buffer (0.25% sodium dodecyl sulfate, 1.9% nonidet P-40, 30 mM Tris-HCl pH 8.0, and 25 mM β-mercaptoethanol) and then boiled for 5 min at 100 °C. The samples were cooled and then peptide:N-glycosidase F (PNGase, Roche Diagnostics GmbH 58,283,321) was added and the reaction mixture was allowed to react overnight at 37 °C according

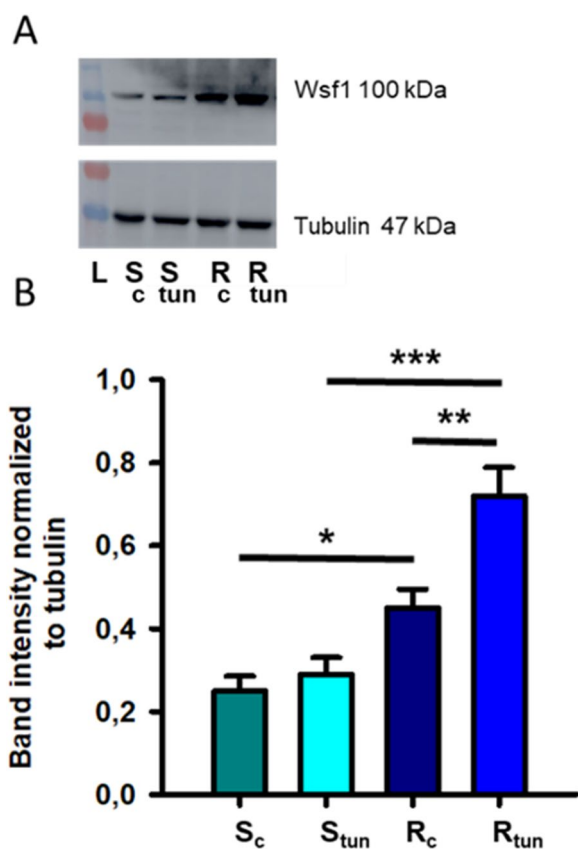


Fig. 2 Changes in the relative content of WFS1 (100 kDa) in S and R cells passaged for 24 h in the absence (c) or presence of Tun (tun 0.1 μ M). **A** Western blot determination of the respective WFS1. Signals for tubulin were used as internal controls. Data are representative of three independent measurements. **B** The optical densities of the protein bands were quantified and are summarized in bar plots. The data are expressed as the mean \pm SD of three independent measurements. Statistical significance: Marked data differ on the level: * $p < 0.05$; ** $p < 0.02$; *** $p < 0.01$

to the manufacturer's instructions. The proportions of both glycosylated and deglycosylated forms of WFS1 proteins were detected by Western blotting with anti-WFS1 antibody.

Results

In the presented research, two variants of murine leukemia cells were used: drug-sensitive parental L1210 cells (S) and derived drug-resistant R cells obtained from S cells by passaging with gradually increasing concentrations of vincristine [29, 38]. If S cells are negative for the measurable presence of *Abcb1* transcript or P-gp (by RT-PCR or Western blotting), R cells contain high levels of either *Abcb1* transcript or P-gp and, in addition, exhibit high resistance (more than 100-fold) to P-gp-substrates (such as vincristine and doxorubicin) compared to S cells (for further details, see Table S1

in supplementary files). Interestingly, R cells tolerate elevated Ca^{2+} concentration in the extracellular space worse than S cells [39]. The massive expression of P-gp in R cells compared to S cells is accompanied by an almost threefold increase in the transcript content of the *Hspa5* gene and a similar increase in the content of its protein product GRP78/BiP (Table S1 in the supplementary files). There is also a very large (over 180-fold) increase in gene expression of the cytochrome P450 family member 2J6 when R and S cells were compared [27].

Expression of *Wfs1* gene in S and R cells

Using the RT-PCR method, we detected the presence of *Wfs1* gene transcripts in S and R cells. These experiments were done after passaging the cells for 24 h under normal conditions and after induction of ERS with either Thap or Tun both at concentration 0.1 μ M (Fig. 1). To verify that the PCR products generated by the PCR reaction under the conditions used and with the designed primers (see Sect. "Protocol used for RT-PCR and qRT-PCRs") actually match the *Wfs1* gene in sequence, we eluted the PCR products from the gel and sent them for sequencing to Eurofins Genomics Germany GmbH (Ebersberg, Germany). The obtained sequence of the PCR products showed an almost complete match with the sequence of the *Wfs1* gene (ID 22393) [40] according to the NCBI gene database (Figure S3 in the supplementary files). It can therefore be concluded that the RT-PCR used reliably detects *Wfs1* gene transcripts in mouse leukemia cells L1210. It seems that there is a difference in the cellular transcript content of the *Wfs1* gene when comparing S and R cells, as the criterion for marginal significance was registered (Fig. 1).

The presence of Tun in the medium during the 24-h passage induces a marked increase in *Wfs1* gene expression in both S and R variants of L1210 cells. The presence of Thap enhances *Wfs1* gene expression more in S cells than in R cells. S cells after passage in the presence of Thap contain significantly more *Wfs1* transcript than R cells.

Levels of WFS1 in S and R cells detected by immunocytochemistry.

First, we detected WFS1 in S and R cells after 24 h passage in the presence and absence of Tun by Western blotting. When detected on the membrane obtained by Western blotting, WFS1 gives a typical 100 kDa protein band [41], which we also detected in S and R cells (Fig. 2).

R cells show a higher cellular WFS1 content than P-gp-negative counterparts do after culture in the absence of Tun. After passage in the presence of Tun, this difference is further accentuated, as we observe a statistically

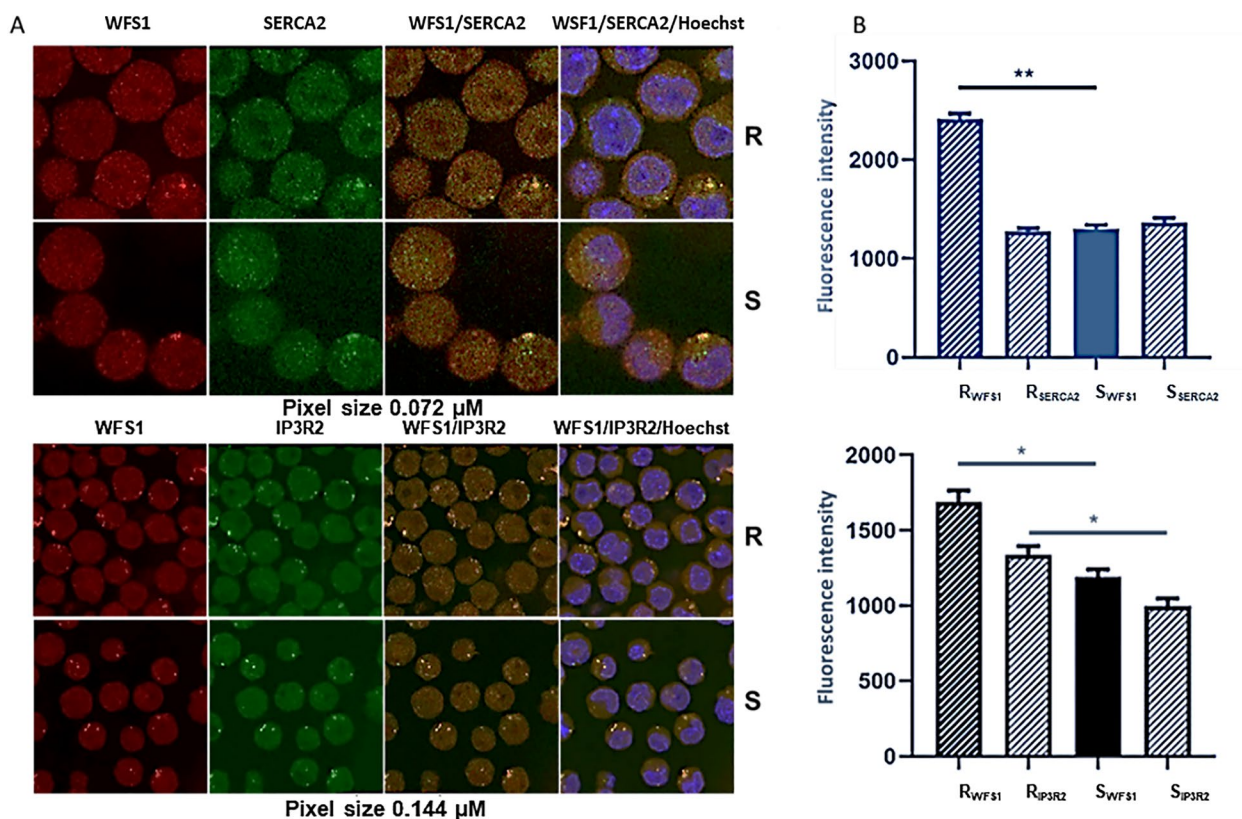


Fig. 3 Immunocytochemical visualization of WFS1 in S and R cells. IP3R2 and SERCA2 were used as ER markers. Rabbit polyclonal anti-WFS1 antibody 26,995-1-AP, anti-SERCA2 monoclonal antibody MA3-910, and anti-IP3R2 monoclonal antibody sc-398434 were used as primary antibodies. Goat anti-rabbit IgG (H+L) coupled to PE-Alexa Fluor™ 647 (A32732, red fluorescence) and goat anti-mouse IgG coupled to Alexa Fluor™ Plus 488 (A32723 green fluorescence) were used as secondary antibodies. In nuclei, dsDNA was labeled with the bisbenzimidazole dye Hoechst 34580 (blue fluorescence [44]). **A** Representative micrographs of S and R cells, labeled with pairs of antibodies against either WFS1 and SERCA2 or WFS1 and IP3R2, along with nuclear labeling using Hoechst 34580, are shown at 5 and 2.5 magnification, respectively, and were analyzed using a Leica TCS SP8 confocal microscope. For magnification 5 and 2.5, xy-scan mode was used with a scan frequency of 700 Hz and 1024 × 1024 and 512 × 512 pixels, respectively. Details are described in Sect. **B** Quantification of red and green fluorescence was achieved by image analysis using ImageJ Fiji software [35]. Green/Red fluorescence of individual cells was assessed in the experiments. Each value is the result of three independent experiments in which a minimum of 22 and a maximum of 47 cells were evaluated. Data are expressed as means ± SD and statistical significance * $p < 0.05$ and ** $p < 0.01$ was obtained using Student's T test

significant increase in WFS1 in R cells and only a slight and statistically insignificant increase in S cells (Fig. 2).

We then used immunocytochemistry to determine the amount and localization of WFS1 in S and R cells passaged in the absence of ER stressors (Fig. 3). As typical ER markers, we chose either the inositol 1,4,5-triphosphate receptor (IP3R), a calcium channel of the ER [42], or the calcium ATPase of sarco(endo)plasmic reticulum (SERCA2), which mediates the reuptake of Ca^{2+} into the ER [43].

The results in Fig. 3 show an increase in WFS1 content in R cells compared to S cells consistently to data on Fig. 2. In contrast, the amount of SERCA2 appears to be the same in S and R cells. This is consistent with previous findings that gene expressions for SERCA2 in R cells are

approximately the same as in S cells (in supplementary data of previous paper [27]). In contrast, the content of IP3R2 is slightly but significantly higher in R than in S cells. When we did IP3R immunocytochemistry with an antibody detecting both IP3R1 and IP3R2 isoforms in S and R cells (16 years ago) and without the use of image analysis, we did not detect significant differences [45]. Figure 3 further indicates that WFS1 is localized in the same structures as IP3R2 and SERCA2. It is best noticeable in the confocal microscope screens where all three fluorescences are merged and the overlay of red and green gives a typical yellow signal [46]. Furthermore, with the Fiji ImageJ software [35], we also evaluated fluorescence intensity from a confocal microscope in S

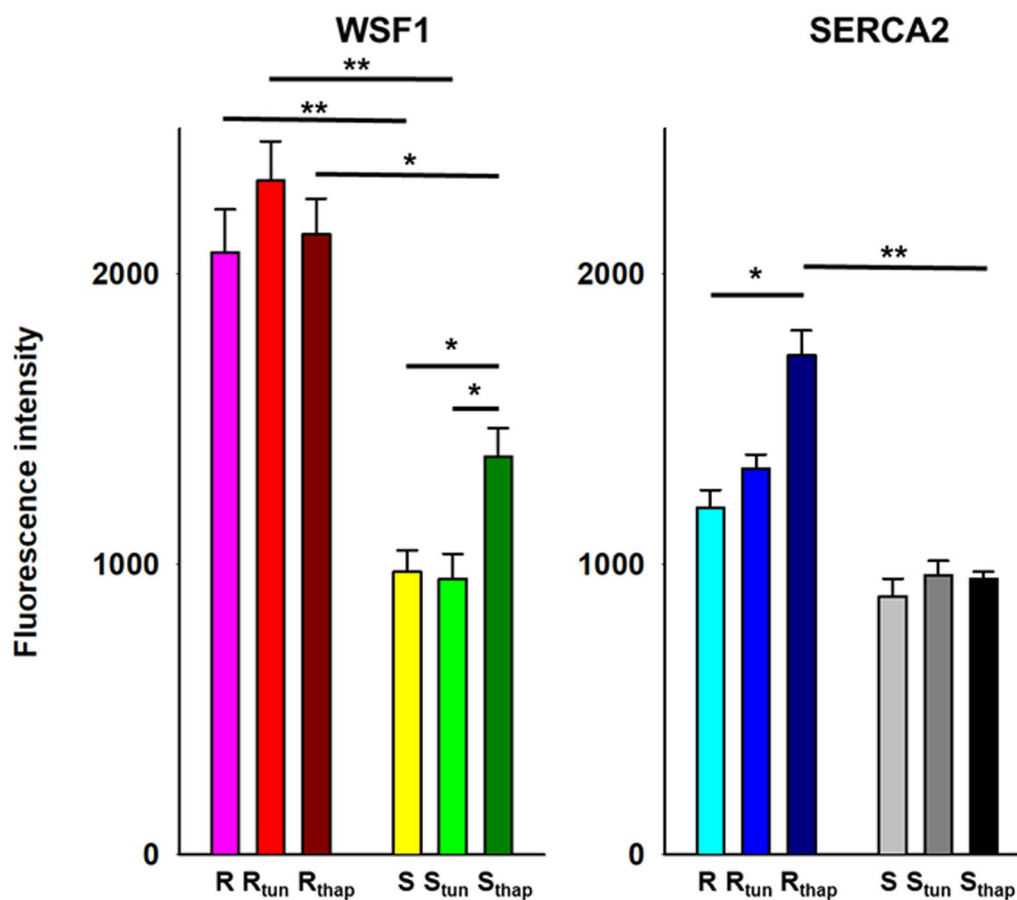


Fig. 4 Quantification of WFS1 and SERCA2 content in S and R cells passaged in the absence and presence of Tun or Thap in concentration 0.1 μ M, which were detected by immunocytochemistry described in Fig. 3. Data are expressed as means \pm SD and statistical significance * $p < 0.05$ and ** $p < 0.01$ was obtained using Student's T test

and R cells passaged for 24 h in the absence and presence of 0.1 μ M Tun or Thap (Fig. 4).

We again confirmed an increased level of WFS1 in R cells compared to S cells. Although the presence of Tun induced an increase in the level of WFS1 in R cells, this did not meet the criterion for statistical significance. After passage with Thap, the level of WFS1 in R cells remained unchanged. The level of WFS1 in S cells did not change after passage with Tun, but after passage with Thap it increased significantly.

Consistent with Fig. 3, the level of SERCA2 is approximately the same in R and S cells. The level of this Ca^{2+} pump increases only in R cells after passage in the presence of Thap, which caused a significant change compared to R cells passaged in the absence of Thap. The different SERCA2 content in R and S cells passaged in the presence of Thap is also significant (Fig. 4).

Expression of several ER markers in S and R cells passaged in the absence or presence of tun or thap

In these experiments, we monitored the expression levels of the genes for following proteins in S and R cells after passaging in the absence and presence of Tun or Thap: ATF6 and PERK as two of the three ER receptors regulating the cellular response to ERS and UPR [47]; GRP78/BiP as a regulator of the cellular response to ERS and UPR [48, 49]; CHOP as a stress-activated proapoptotic protein active in the ERS [50]; and mRNA for *Xbp1* and its spliced variant *sXbp1*, which is generated by IRE1 mediated splicing of *Xbp1* mRNA and encodes a transcription factor active in the ERS [51].

Next, we detected ATF6 protein levels in S and R cells by Western blotting after passaging in the absence and presence of Tun or Thap. Here, we detected and quantified its full-length 90 kDa form, which is an integral protein of the ER membrane. Furthermore, we also detected a 50 kDa proteolytic fragment of ATF6, which, as a transcription factor, regulates a specific

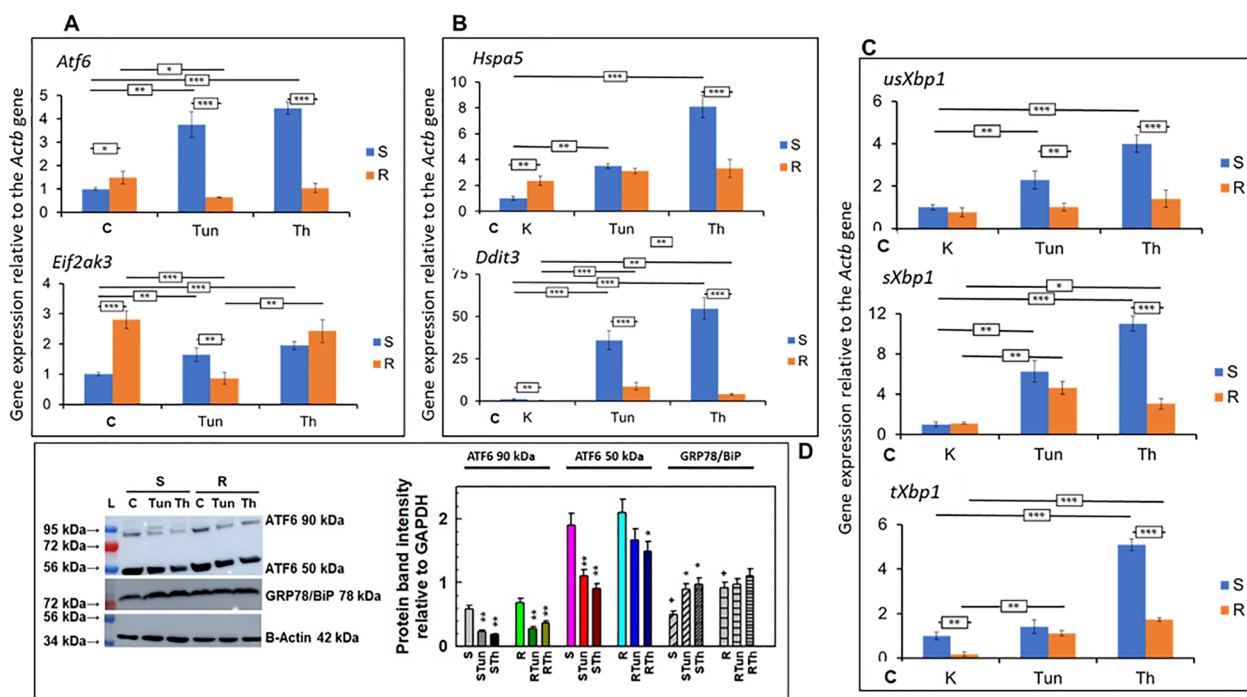


Fig. 5 Detection and quantification of transcripts of genes encoding ATF6 (*Atf6*), PERK (*Eif2ak3*), GRP78/BiP (*Hspa5*), CHOP (*Ddit3*) and variants of XBP1 (*usXbp1*—unspliced *Xbp1* mRNA, *sXbp1*—spliced *Xbp1* mRNA and *tXbp1* both variants of *Xbp1* mRNA, primers for *Xbp1* were designed to recognize these three categories [32]) by qRT-PCR (using primers listed in Table 1) (A–C) and detection of the 90 kDa and 50 kDa variants of ATF6 by Western blot (D). S and R cells were passaged once in the absence or presence of Tun or Thap. Transcript levels were normalized to the housekeeping gene β -actin and are expressed as the means \pm SD of three independent measurements. The membranes derived from Western blotting are representative of three independent measurements. Protein bands for 90 kDa ATF6 were quantified by densitometry, expressed as means \pm SD and were documented in the bar graph. Significance: data are higher than in S cells at * $p < 0.05$, ** $p < 0.01$ and *** $p < 0.001$

transcriptional response of ERS [52]. The results are documented in Fig. 5.

R cells also differ from S cells by slightly higher expression of the *Atf6* gene and much higher expression of the *Eif2ak3* gene encoding PERK (Fig. 5A). While in S cells *Atf6* gene expression is significantly increased after passage in the presence of both ER stressors (Tun and Thap), in R cells it either remains at the control value after passage in the presence of Thap or even decreases after passage in the presence of Tun. *Eif2ak3* gene expression is increased in S cells after passage in both ER stressors (Tun and Thap), but to the lower extent than the *Atf6* gene (Fig. 5A). The presence of Tun during passage of R cells induces a marked reduction in *Eif2ak3* gene expression to the extent that its level is lower than in S cells under the same conditions (Fig. 5A). Passage of R cells in the presence of Thap induces only a non-significant decrease in *Eif2ak3* gene expression. The expression of the *Hspa5* gene encoding GRP78/BiP is higher in P-gp-positive R than in P-gp-negative S cells (Fig. 5B), which is consistent with the results published in previous articles [27, 28]. Passage of S cells in Tun and Thap induced more

than a threefold and more than an eightfold increase in expression of this gene. In contrast, *Hspa5* gene expression in R cells remains approximately at the same level after passage in Tun or Thap. This causes that, after passage of S and R cells in Tun, both variants show approximately the same expression of the *Hspa5* gene, and after passage in Thap the expression of this gene in S cells is significantly higher than in R cells (Fig. 5B).

Expression of the *Ddit3* gene encoding CHOP is low in unstressed S and R cell variants (i.e., passaged in the absence of Tun or Thap, Fig. 5B). This is in agreement with the notion that CHOP plays a role in inducing apoptosis in cells under ERS [53], and thus its expression is not required in the absence of stressors. However, in agreement with previous work [28], a significantly lower level of expression of *Ddit3* is detected in R than in S cells. Passage of S cells in the presence of Tun or Thap induced a more than 30-fold and more than 50-fold increase in *Ddit3* gene expression, respectively (Fig. 5B). In contrast, *Ddit3* gene expression increases more modestly in R cells (less than tenfold) after passage in the presence of Thap and Tun (Fig. 5B).

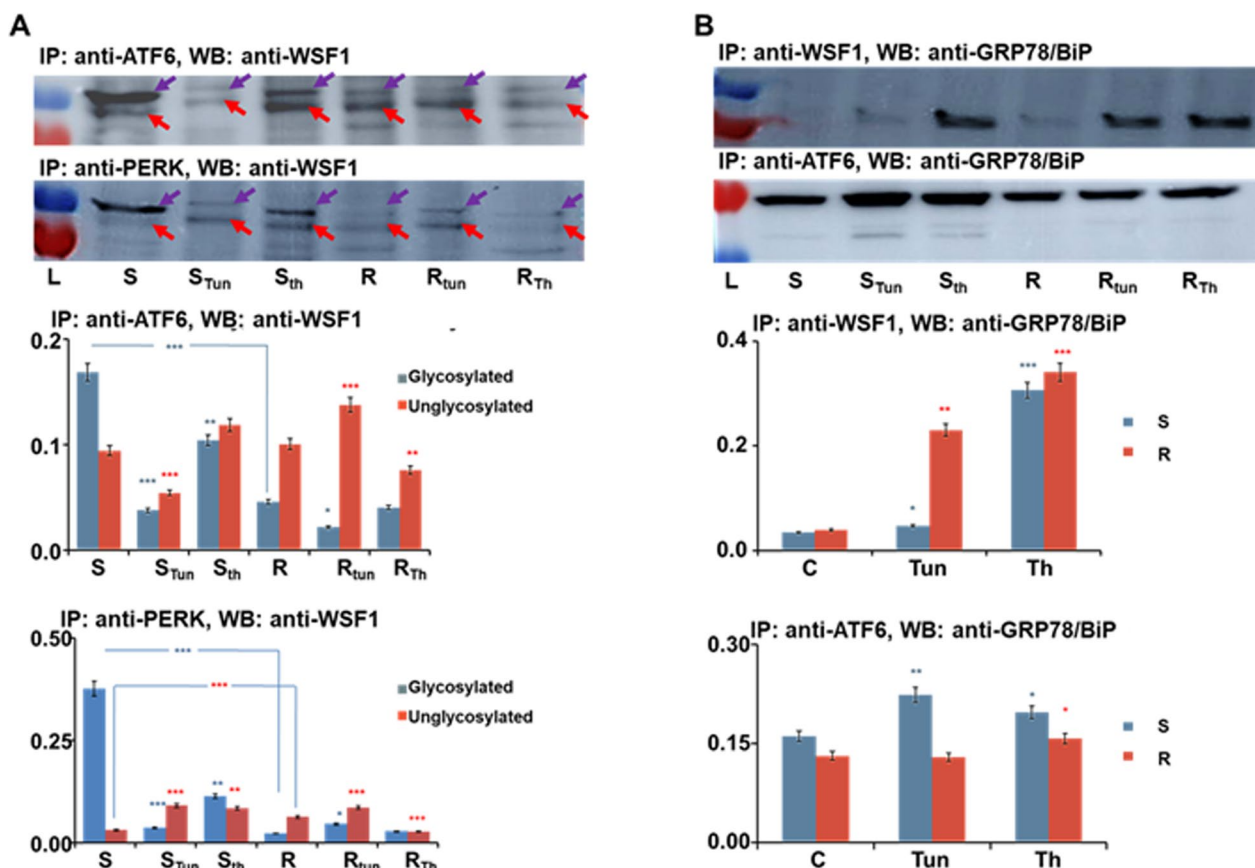


Fig. 6 Detection of protein: protein interaction by immunoprecipitation. S and R cells were passaged in the presence or absence of either Tun or Thap for 24 h, and then cells were harvested, homogenized, and used for immunoprecipitation (see Sect. "Immunoprecipitation Procedure"). **A** Cell homogenates immunoprecipitated with anti-ATF6 or anti-PERK antibody were detected on a Western blot membrane with anti-WSF1 antibody. Protein bands for glycosylated WSF1 (purple arrows) and unglycosylated WSF1 (red arrows) are visible on the blots. Protein bands were quantified by densitometry and protein amounts are documented in bar plots. **B** Cell homogenates immunoprecipitated with anti-WSF1 or anti-ATF6 antibody were detected on Western blot membrane with anti-GRP78/BiP antibody. Protein bands were quantified by densitometry and protein amounts are documented in bar plots. Western blots of membranes are representative of three independent measurements. Data in bar graphs are expressed as mean \pm SD of three independent experiments. Statistical significance: * $p < 0.05$, ** $p < 0.02$, *** $p < 0.01$

The presence of unspliced and spliced *Xbp1* gene transcript is not significantly different in S and R cells (Fig. 5C). Passaging in the presence of Tun or Thap led to an elevation of the spliced transcript in both cell variants, but more largely in S than in R cells. The amount of unspliced transcript increases after passage in Tun or Thap only in S cells. These data suggest a reduced

requirement for the transcription factor resulting from translation of *sXbp1* mRNA in R cells as compared to S cells. A qRT-PCR with primers not discriminating between *sXbp1* and *usXbpi* shows a higher signal in S than in R cells after passage in the absence of Tun and Thap (Fig. 5C). Passage in the presence of Tun induces a significant signal increase in R but not in S cells. Passage in the presence of Thap induces growth in both cell variants, but more pronounced in S.

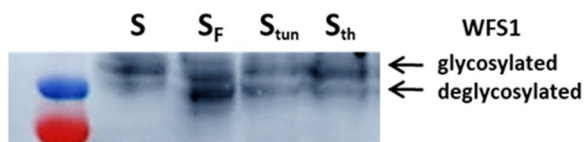


Fig. 7 Detection of protein bands with immunoreactivity to anti-WSF1 antibody in untreated cells (S), cells treated with PNGase (S_F), and bands after passaging with Tun (S_{Tun}) or Thap (S_{Th})

Western blotting revealed an approximately equal level of the 90 kDa variant of ATF6 protein in S and R cells (Fig. 5D). If cells were passaged in the presence of Tun or Thap, the level of this variant decreased in both S and R cells. We also detected the 50 kDa version of ATF6 and its level seems to decrease after passage with Tun or Thap in both S and R cells. In contrast, the protein level of GRP78/BiP is higher in R than in S cells. The

amount of this protein increases under conditions of ER stress induced by Tun or Thap in S cells, but remains unchanged after treatment with Tun and Thap.

Complex formation between WFS1 and proteins active in ERS detected by immunoprecipitation

We used immunoprecipitation to detect protein: protein interaction. In homogenates from S and R cells passaged in the presence of Tun or Thap, we immunoprecipitated proteins with an antibody against ATF6 and PERK. We subjected the isolated immunoprecipitates to SDS-PAGE followed by Western blotting using an anti-WFS1 primary antibody (Fig. 6A). We detected two separate protein bands in the 100 kDa region that could correspond to the glycosylated and unglycosylated forms of WFS1 [18]. To prove this, we subjected S cells to peptide:N-glycosidase F (PNGase, EC 3.5.1.52) treatment and compared the molecular masses of the protein bands from cells treated in this way with untreated S cells and S cells passaged with Tun and Thap on Western blots with anti-WFS1 antibody (Fig. 7). When comparing untreated S cells with PNGase-treated cells, we observed an accentuation of a protein band with a lower molecular weight and therefore attributed it to the deglycosylated form of WFS1. A similar decrease in molecular weight after deglycosylation with PNGase was also observed by Takeda et al. [54]. After passaging S cells with Tun or Thap, we observed an increase in the protein band for deglycosylated WFS1, but to a lower level than when using PNGase.

When lysates from S cells were immunoprecipitated with anti-ATF6 or anti-PERK after passage in medium in the absence of an ER stressor, the glycosylated form of WFS1 predominated. However, this was visibly reduced in R cells treated and immunoprecipitated in the same way. Tun, which directly suppresses N-glycosylation of proteins in the ER [12], significantly reduced the amount of glycosylated WFS1 in both S cell immunoprecipitates obtained with anti-ATF6 or anti-PERK antibody. In immunoprecipitates from R cells after passage in the presence of Tun, we observed a reduction of the glycosylated form of WFS1 only when using an anti-ATF6 antibody, and on the contrary, when using an anti-PERK antibody, the amount of the glycosylated form paradoxically seemed to be higher (Fig. 6A).

Thap, which by inhibiting SERCA blocks the reuptake of Ca^{2+} into the ER and thus causes its calcium depletion, disables the calcium-dependent function of both calnexin and calreticulin, which are essential for glycosylation in the ER [10, 11]. In addition, Thap during the passage of S cells significantly reduces the amount of glycosylated WFS1 in both immunoprecipitates obtained by

anti-ATF6 or anti-PERK antibody (Fig. 6A). However, Thap does not change the amount of glycosylated WFS1 in R cell immunoprecipitates regardless of whether anti-ATF6 antibody or anti-PERK antibody was used.

Overall, it can be concluded that the amount of total WFS1 (sum of glycosylated and non-glycosylated form) in complex with ATF6 or PERK is higher in S cells than in R cells after passage in the absence of Thap and Tun (Fig. 6A). After culturing S cells in the presence of Tun or Thap, the total amount of WFS1 complexes with ATF6 and PERK decreases. In R cells, the decrease in the glycosylated WFS1 form in complexes with ATF6 and PERK appears to be replaced by an increase in the non-glycosylated form after passage with Tun. On the contrary, after passage of R cells in the Thap containing medium, there is a decrease in the amount of total WFS1 in the complex with these ER receptors (Fig. 6A).

After immunoprecipitation of cell lysates with anti-WFS1 antibody and detection and anti-GRP78/BiP antibody, we detected an increase in the complex formed by these proteins in both S and R cells passaged in the presence of Tun or Thap (Fig. 6B). However, while a large increase in the formation of this complex was observed in R cells after passage with both Tun and Thap, in S cells this occurs only after passage with Thap and only a slight but statistically significant increase is obtained after passage with Tun. The increase in complex formation between GRP78/BiP and WFS1 is more pronounced in R cells than in S cells after passaging in the presence of Tun and Thap. After passage of cells in the absence of Tun and Thap, the amount of the complex between these two proteins is at the limit of detectability under our conditions in both S and R cells.

After immunoprecipitation of cell lysates with anti-ATF6 antibodies and detection and anti-GRP78/BiP antibody, we detected an increase in the complex formed by these proteins in S cells passaged in the presence of Tun or Thap (Fig. 6B). In contrast, in R cells there was only a slight increase in the amount of this complex in the immunoprecipitate only when they were passaged in the presence of Thap but not in the presence of Tun.

Discussion

The major finding of this work is that R cells with multi-drug resistance conferred by the presence of P-gp show increased expression of the gene *Wfs1* encoding wolframin, an integral ER protein, at both the mRNA and protein levels (Figs. 1, 2, 3 and 4). Information on such co-expression is lacking to date. WFS1 is known to be involved in ER action in modulating intracellular calcium homeostasis [20, 21]. We have previously described that R cells are more sensitive to increases in extracellular matrix Ca^{2+} ion concentrations, which is likely related

to an increased ability to uptake $^{45}\text{Ca}^{2+}$ from the external environment when comparing R and S cells [39]. This led us to believe that R cells compared to S cells have altered intracellular calcium regulation [55]. The increased expression of WFS1 as another player in the regulation of calcium ion homeostasis is probably also involved in the changes observed in R cells. Moreover, WFS1 is also involved in the regulation of the UPR and is thought to antagonize ERS [23]. Consistent with this, R cells, which express more WFS1 than S cells (Figs. 1, 2, 3 and 4), are less sensitive to ER stressors such as Tun [27, 28] or Thap [27, 45]. After passage with both Tun and Thap, *Wfs1* gene transcription increased in both S and R cells (Fig. 1). However, there is no such clear increase in WFS1 protein levels under the influence of Tun or Thap, which should reflect increased transcription of the *Wfs1* gene (Figs. 3 and 4). A small increase in WFS1 protein level under the influence of Tun was registered in R cells but not in S cells (Fig. 2). Thus, the increase in WFS1 transcript levels in S cells after culture with Tun (Fig. 1) was not reflected in increased WFS1 protein levels (Figs. 2 and 4), which is consistent with the findings of Yamaguchi et al. [19]. These authors showed that inhibition of N-glycosylation by Tun increased WFS1 mRNA levels but not protein levels. However, we observed a significant increase in WFS1 protein in R cells. This discrepancy may be explained by further speculation. In previous work, we demonstrated that R cells exhibit an altered response to ER stress, wherein, after N-glycosylation was blocked, unglycosylated [56] and ubiquitinated [57] P-gp continued to mature and integrate into membranes, maintaining its transport function. This unconventional pathway may be attributed to the increased GRP78/BiP levels in these cells, which confer resistance to ER stress [28]. WFS1, as a regulator of calcium traffic between ER and cytosol [21], could participate in the already described increased sensitivity of R cells to the elevation of Ca^{2+} concentration in the extracellular matrix [39] or in the change of calcium homeostasis in R cells compared to S cells [55]. However, its action on calcium homeostasis may not be limited only to the ER, because a decrease in the (Na^+ - Ca^{2+}) exchanger expression was found in myocytes of the left ventricle of the heart from WFS1-deficient mice (*Wfs1-e5/-e5*) as compared with wild type [58].

In agreement with previous articles [27, 28], gene expression of *Atf1*, *Eif2ak3* (encoding ATF1 and PERK) and *Hspa5* (encoding GRP78/BiP) is higher in R cells than in S cells (Fig. 5). R and T cells respond to the presence of Tun or Thap genes by differentially expressing these three genes. While their expression increases in S cells, rather a decrease or unchanged level of expression is observed in R cells.

Relatively little expression of the *Ddit3* gene (encoding CHOP), a transcription factor inducing the predominance of pro-death stimuli during ERS [59], was found in S and R cells (although significantly lower in R cells) passaged in the absence of Tun and Thap (Fig. 5). The presence of Tun or Thap during S cell passage induces a large increase in the expression of this gene, respectively. This indicates an onset of ERS induced cell death processes [60]. On the other hand, when comparing R cells with S cells, a significantly reduced increase in the expression of this gene was observed after its induction by passaging the cells in the presence of Tun or Thap (Fig. 5). Thus, Tun or Thap induced weaker ERS in R than in S cells. The weaker induction of ERS by Tun and Thap in R cells compared to S cells can also be deduced from the increase in the spliced form of the *sXbp1* transcript in R cells compared to that in S cells after passage with these ER stressors (Fig. 5). This spliced form, resulting from the splicing of *usXbp1* with activated IRE1 (a third ER stress receptor), encodes a functional transcription factor active in the ERS [61]. The induction of the transcription factor *usXbp1* is ensured by ATF6 and thus is regulated by ATF6 at the level of transcription and by IRE1 at the level of further processing of the transcript [61]. Therefore, to complete the mosaic of regulatory events in ERS induced by Tun and Thap in R and S cells, it was also necessary to measure changes in ATF6 expression at the protein level. This analysis revealed a decrease in the 90 kDa form of ATF6 after passage of S and R cells with Tun or Thap compared to cells passaged in the absence of these ER stressors (Fig. 6D). This would suggest that ATF6 might be proteolytically cleaved into a 50 kDa transcription factor active in the ERS [52]. We detected the presence of the 50 kDa form of ATF6, which was, however, paradoxically downregulated by the influence of Tun and Thap (Fig. 6D), i.e. in ERS conditions, when it should rather increase. This may be related to the fact that WFS1 acts under ERS induced in S and R cells with Tun and Thap. WFS1 has been described to counteract the development of ERS by promoting the ubiquitination and subsequent proteasomal degradation of ATF6 and thus promoting the elimination of this protein [62]. WFS1 as a negative regulator of ERS was also confirmed by a recent results of Gong et al. [63] that the cellular content of ATF6, GRP78/BiP, XBP1 and CHOP increases with *WFS1* gene silencing and, conversely, decreases after transfection with a plasmid carrying *WFS1* gene.

After passage of S cells in the absence of the ER stressors Tun and Thap, we detected by immunoprecipitation WFS1 predominantly in the glycosylated form in a complex with the ER stress receptors ATF6 and PERK (Fig. 6A). These receptors are blocked with GRP78/BiP under conditions without ERS, and at the same time

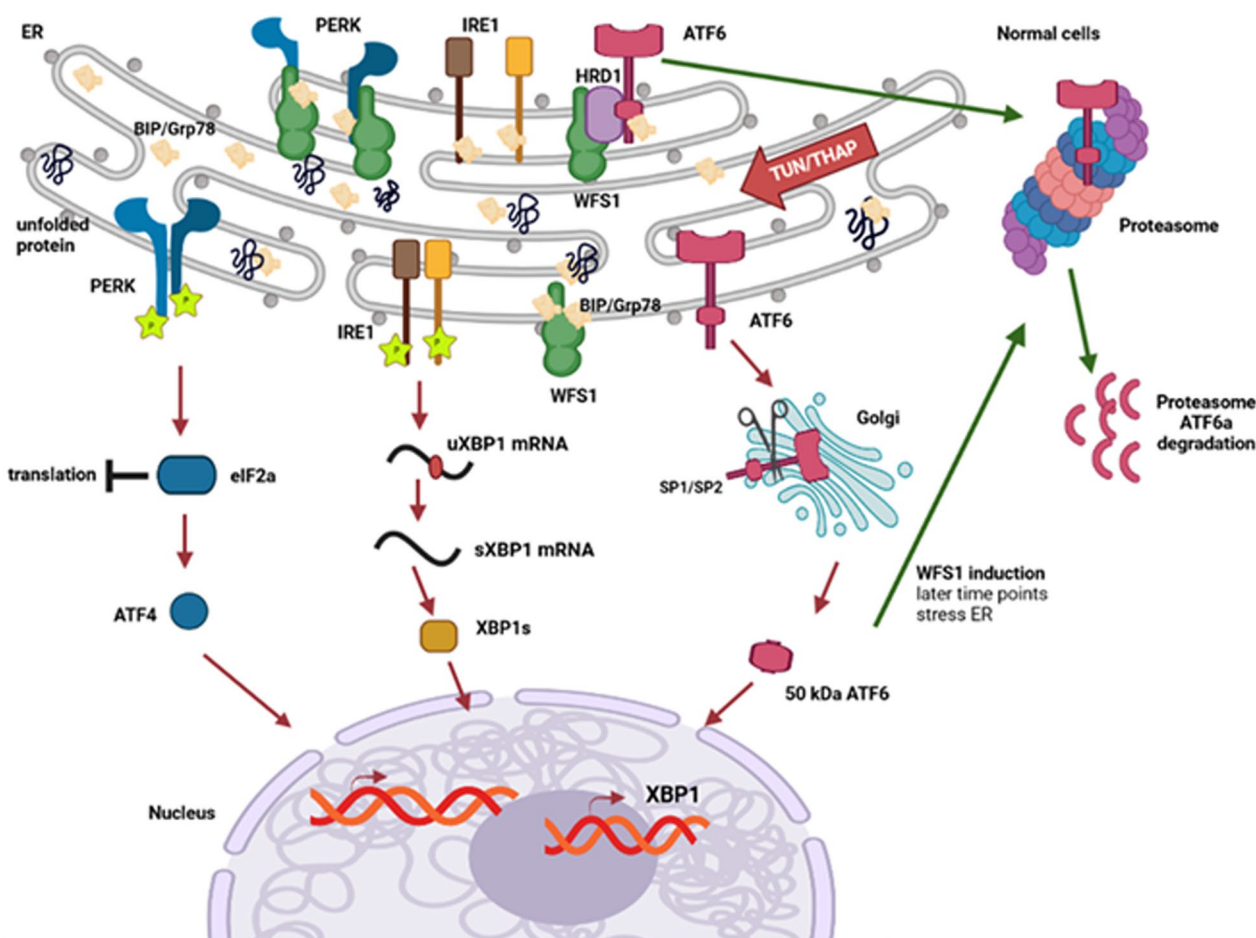


Fig. 8 Schematic summary of pathways that interfere with cellular homeostasis during ERS, including the role of WFS1. Under normal conditions, the stress receptors ATF6 and PERK are inactivated by binding to GRP78/BiP [13]. Under these conditions, WFS1 is also bound to these receptors (Fig. 6A) and can inactivate them. Upon addition of Tun or Thap, the ERS begins to develop, resulting in the accumulation of unfolded proteins in the ER lumen [11, 12]. Under these circumstances, GRP78/BiP preferentially binds to unfolded proteins and begins to leave IRE1, ATF6 and PERK [13]. In addition, WFS1 is released from binding to PERK and ATF6 while preferring binding to GRP78/BiP (Fig. 6B). We do not yet know the exact function of the formation of the GRP78/BiP and WFS1 complex that we detected in Fig. 6B. Under ERS conditions, three pathways are initiated: i. PERK tetramerizes, undergoes autophosphorylation, and phosphorylates eIF2α [72]. This phosphorylation prevents heterotrimeric formation from eIF2 α, β, and γ subunits. Lack of this trimer reduces the level of overall translation. If the reduced level of ERS translation does not dampen, CHOP transcription is activated through the expression of ATF4 (activating transcription factor 4). CHOP then induces apoptosis in the cell [72]. Elevation of larger amount of *Ddit3* transcript (encoding CHOP) in S cells and lower amount in R cells after passage in the presence of Tun or Thap is documented on Fig. 5B. ii. ATF6 is released from the ER membrane and translocated to the Golgi apparatus, where it is proteolytically cleaved and a 50-kDa transcription factor is formed, which binds to DNA and induces the transcription of GRP78/BiP, XBP1 and unfolded protein cleavage enzymes. However, elevation of WFS1 promotes ubiquitination and proteasomal degradation of ATF6, which counteracts ERS activation by ATF6. iii. IRE1 homodimerizes and phosphorylates, allowing manifestation of RNA splicing activity [73]. RNA splicing activity of IRE1 processes specific splicing of *uXBP1* mRNA, transcribed by induction with 50 kDa ATF6, to *sXbp1*. Translation of *sXbp1* produces a functional XBP1s transcription factor that initiates the expression of ER-associated protein degradation (ERAD) genes. The scheme was created using the online graphic software Biorender (Toronto, Ontario, Canada)

WFS1 is also bound to them, as shown schematically in Fig. 8. Passage of S cells in the presence of Tun and Thap significantly reduces the amount of the glycosylated form of WFS1 in complex with ATF6 and PERK. We also detected changes in the amount of the non-glycosylated form of WFS1 in complexes with these receptors after passaging of S cells with Tun or Thap, but they were less

pronounced (Fig. 6A). In R cells, there is a smaller amount of the glycosylated form of WFS1 in complexes with ATF6 and PERK than in S cells, and the non-glycosylated form appears to predominate in the complexes. We previously documented several aberrations in protein N-glycosylation in P-gp positive variants of L1210 cells compared to P-gp negative counterparts [38, 64–66].

A decrease in the proportion of glycosylated to non-glycosylated form of WFS1 in complexes with ATF6 and PERK may belong to them. If we sum the amounts of glycosylated and non-glycosylated forms of WFS1 that were in complexes with either ATF6 or PERK and compare them in S and R cells (Fig. 6A), we found more WFS1 in complexes in S cells than in R cells. Interestingly, the expression level of WFS1 is higher in R cells than in S cells, both at the mRNA (Fig. 1) and protein level (Fig. 2). In P-gp positive cells, the non-glycosylated form of WFS1 appears to be predominant and forms functional complexes with the partner proteins ATF6 and PERK even after passages in the absence of ER stressors (Fig. 6A). However, N-glycosylation is thought to be essential for WFS1 biogenesis and stability, and aberrations in WFS1 glycosylation can disrupt its proper functions [18, 19]. Data on Fig. 6A indicated that there appears to be a way for this protein to remain functional in R cells despite the immature low-glycosylated form, in which it occurs in complexes with PERK and ATF6. It may be related to the fact that in P-gp positive variants of L1210 cells, proteins can escape proteasome degradation when N-glycosylation in ER is suppressed. An example of this feature can be P-gp, which after repeated passages with Tun was present in a non-glycosylated [56] and even ubiquitinated [57] form in the plasma membrane, where it retained its transport activity. Visual changes in protein bands on Western blot membranes of immunoprecipitates obtained from R cells after passaging in the absence or presence of Tun or Thap are less pronounced than in S cells, but quantification provided statistical significance of the differences (Fig. 6A).

Taking into account all the above facts, we can conclude that apart from GRP78/BiP, which is generally known to block the function of the stress receptors IRE1, PERK and ATF6 (Fig. 8) in conditions without ERS [67], the last two receptors are in complex with WFS1. Similar to GRP78/BiP, WFS1 appears to dissociate from association with PERK or ATF6 when ER stressors induce ERS (Fig. 8). The function of WFS1 binding to both ER stress receptors is not yet elucidated. However, if we accept the role of WFS1 as a protein suppressing ERS through the degradation of ATF6 [52, 62], and also that WFS1 dissociates from ATF6 and PERK under ERS conditions (Fig. 6A), then it is reasonable to assume that WFS1, by analogy with GRP78/BiP, exerts a blocking effect on both receptors when bound to them. Thus, there is a possibility that WFS1 suppresses ERS by simultaneously blocking these stress receptors and inducing ATF6 degradation.

If the cell homogenates of S and R cells after passage in the absence of any ER stressor were subsequently immunoprecipitated with an anti-WFS1 antibody and detected with an anti-GRP78/BiP antibody, almost no presence of

the complex of these two proteins was detected (Fig. 6B). Interestingly, after passage in the presence of either Tun or Thap, the immunoprecipitate contained considerably increased amounts of GRP78/BiP in complexes with WFS1. The presence of these complexes seems to be always higher in R cells than in S cells at passages without and with ER stressors. This indicated that both GRP78/BiP and WFS1 leaves ATF6 and PERK during ERS induced by Tun and Thap in common complex (Fig. 8).

Our results showed for the first time the possibility of complex formation between WFS1 and ERS proteins, either ATF6 and PERK, which is repressed by ERS (Fig. 6A), or GRP78/BiP, which is promoted by ERS (Fig. 6B). Thus, ATF6, PERK (Fig. 6A) and GRP78/BiP (Fig. 6B) are other three ER proteins that co-immunoprecipitate with WFS1 in addition to Sarco(endo)plasmic reticulum ATPase described by Zatyka et al. [68]. The ability of WFS1 to form immunoprecipitable complexes with partner proteins is not limited to those that are ER residents. Such interactions with Vacuolar-type H1-ATPase V1A subunit [69], Ca^{2+} /CaM complex [70] and Na⁺/K⁺ATPase β 1 subunit [71] have been described.

Immunoprecipitates from S and R cells after their passage in the absence of ER stressors, which were obtained with the anti-ATF6 antibody, contain complexes of ATF6 and GRP78/BiP detected with antibody against GRP78/BiP (Fig. 6B). This is consistent with the idea that this receptor and other two receptors of ER (PERKs and IRE1) are under normal conditions inactivated through association with GRP78/BiP [13] (Scheme on Fig. 8). The presence of Tun and Thap during passage induces the accumulation of unfolded proteins in the ER, leading to ERS [11, 12]. Under these conditions, unfolded proteins should compete with ATF6, PERK, and IRE1 for binding to GRP78/BiP, which then leaves them, allowing activation of all three receptors [13]. Contrary to this notion, after passage of S and R cells in the presence of Tun and Thap, more GRP78/BiP was found in complex with ATF6 (Fig. 6B). We do not yet have a relevant explanation for this contradiction. However, certain indications allow the following speculation. The association between ATF6 and GRP78/BiP appears to be stable, arguing against simple competition with unfolded proteins as the mechanism controlling the release of GRP78/BiP from ATF6 [74]. These authors supposed that ER stress-induced GRP78/BiP release is ensured by specific sequences in ATF6 that activate GRP78/BiP dissociation. Therefore, the process of this dissociation may not be simple and may be limited by various factors. Such a factor may be the over-expression of WSR1 (Fig. 1) in S and R cells under conditions of ERS induced with Tun or Thap. This protein promotes ubiquitination and proteasomal degradation of ATF6 [62],

while it can be guided by Grp78/BiP as a chaperone in this way.

For a clearer summary of the acquired knowledge, we created a scheme in Fig. 8. In conditions without ERS, ATF6, PERK and IRE1 receptors are blocked with GRP78/BiP. We also demonstrated immunoprecipitable binding with WFS1 for ATF6 and PERK. Under conditions of ERS induced by either Tun or Thap, GRP78/BiP is released from complexes with ATF6, PERK and IRE1, and WFS1 is released from complexes with ATF6 and PERK. Both WFS1 and GRP78 can co-exist in a co-immunoprecipitable complex (Fig. 8). This leads to: i. the activation of PERK resulting in the slowing down of overall translation and, through ATF4, the induction of ERS response enzymes; ii. the activation and proteolytic cleavage of ATF6 resulting in the induction of the Xbp1 gene; iii. the activation of IER1 resulting in the specific splicing of *usXbp1* RNA to *sXbp1* RNA, the translation of which creates a transcription factor active in responses to ERS. Cellular overproduction of WFS1 results in increased ubiquitination and proteosomal degradation of ATF6. The latter regulatory effect of WFS1 operates against the development of ERS.

Conclusions

In the presented work, we demonstrated increased expression of WFS1 in leukemic cells with multidrug resistance mediated by P-gp (Figs. 1, 2, 3). In these cells, we have previously shown that P-gp overexpression is accompanied by an altered response to ERS induced with Tun or Thap. WFS1 as an ER resident protein is known to suppress ERS development. In the present work, we provide evidence that WFS1 is able to form complexes with ER receptors (ATF6 and PERK, Fig. 6A) in conditions without ERS and with the central regulator of the cell response to the UPR (GRP78/BiP Fig. 6B) in conditions of ERS induced with Tun and Thap. For the first time, we brought data pointing to the participation of WFS1 in ensuring the resistance of P-gp positive cells to Tun and Thap.

Supplementary Information

The online version contains supplementary material available at <https://doi.org/10.1186/s12935-025-03661-w>.

Supplementary material 1.

Author contributions

Conceptualization, Z.S., A.B.; funding acquisition, Z.S., A.B. and M.S.; data curation, S.K., L.P., M.S.; supervision, Z.S., A.B., investigation, S.K., L.P., M.S. V.B.; methodology, S.K., L.P., M.P., A.B., Z.S.; writing—original draft preparation, S.K., L.P., M.S.; project administration, L.P., M.S., V.B. J.S.; writing—review and editing, Z.S. and A.B., J.S.. All authors have read and agreed to the published version of the manuscript.

Funding

This research was funded by the Grant Agency of the Ministry of Education of the Slovak Republic and the Slovak Academy of Sciences (grants VEGA-2/0141/22, VEGA-2/0030/23 and VEGA-2/0046/24).

Data availability

The authors declare that all data supporting the results of this study are available in the paper and in the Supplementary Information. Raw data are available upon request from the corresponding author.

Declarations

Institutional review board statement

Not applicable.

Informed consent

Not applicable.

Competing interests

The authors declare no competing interests.

Author details

¹Institute of Molecular Physiology and Genetics, Centre of Biosciences, Slovak Academy of Sciences, Dúbravská Cesta 9, 840 05 Bratislava, Slovakia. ²Institute of Biology, Faculty of Medicine and Dentistry, Palacký University Olomouc, Hněvotínská 3, 775 15 Olomouc, Czechia. ³Institute of Biochemistry and Microbiology, Faculty of Chemical and Food Technology, Slovak University of Technology in Bratislava, Radlinského 9, 81237 Bratislava, Slovakia.

Received: 28 March 2024 Accepted: 24 January 2025

Published online: 07 February 2025

References

- Pavlikova L, Seres M, Breier A, Sulova Z. The roles of microRNAs in cancer multidrug resistance. *Cancers*. 2022;14(4):1090.
- Breier A, Gibalova L, Seres M, Barancik M, Sulova Z. New insight into p-glycoprotein as a drug target. *Anticancer Agents Med Chem*. 2013;13(1):159–70.
- Juliano RL, Ling V. A surface glycoprotein modulating drug permeability in Chinese hamster ovary cell mutants. *Biochim Biophys Acta*. 1976;455(1):152–62.
- Nanayakkara AK, Follit CA, Chen G, Williams NS, Vogel PD, Wise JG. Targeted inhibitors of P-glycoprotein increase chemotherapeutic-induced mortality of multidrug resistant tumor cells. *Sci Rep*. 2018;8(1):967.
- Petrou T, Olsen HL, Thrasivoulou C, Masters JR, Ashmore JF, Ahmed A. Intracellular calcium mobilization in response to ion channel regulators via a calcium-induced calcium release mechanism. *J Pharmacol Exp Ther*. 2017;360(2):378–87.
- Braakman I, Hebert DN. Protein folding in the endoplasmic reticulum. *Cold Spring Harb Perspect Biol*. 2013;5(5):a013201.
- Victor P, Sarada D, Ramkumar KM. Crosstalk between endoplasmic reticulum stress and oxidative stress: focus on protein disulfide isomerase and endoplasmic reticulum oxidase 1. *Eur J Pharmacol*. 2021;892:173749.
- van Vliet AR, Garg AD, Agostinis P. Coordination of stress, Ca²⁺, and immunogenic signaling pathways by PERK at the endoplasmic reticulum. *Biol Chem*. 2016;397(7):649–56.
- Hebert DN, Molinari M. In and out of the ER: protein folding, quality control, degradation, and related human diseases. *Physiol Rev*. 2007;87(4):1377–408.
- Wang Q, Groenendyk J, Michalak M. Glycoprotein quality control and endoplasmic reticulum stress. *Molecules*. 2015;20(8):13689–704.
- Sehgal P, Szalai P, Olesen C, Praetorius HA, Nissen P, Christensen SB, Engedal N, Moller JV. Inhibition of the sarco/endoplasmic reticulum (ER) Ca(2+)-ATPase by thapsigargin analogs induces cell death via ER Ca(2+) depletion and the unfolded protein response. *J Biol Chem*. 2017;292(48):19656–73.

12. Banerjee A, Lang JY, Hung MC, Sengupta K, Banerjee SK, Baksi K, Banerjee DK. Unfolded protein response is required in nu/nu mice microvasculature for treating breast tumor with tunicamycin. *J Biol Chem*. 2011;286(33):29127–38.
13. Bertolotti A, Zhang Y, Hendershot LM, Harding HP, Ron D. Dynamic interaction of BiP and ER stress transducers in the unfolded-protein response. *Nat Cell Biol*. 2000;2(6):326–32.
14. Walter F, O'Brien A, Concannon CG, Dussmann H, Prehn JHM. ER stress signaling has an activating transcription factor 6alpha (ATF6)-dependent "off-switch." *J Biol Chem*. 2018;293(47):18270–84.
15. Fribley A, Zhang K, Kaufman RJ. Regulation of apoptosis by the unfolded protein response. *Methods Mol Biol*. 2009;559:191–204.
16. Hano M, Tomasova L, Seres M, Pavlikova L, Breier A, Sulova Z. Interplay between P-Glycoprotein expression and resistance to endoplasmic reticulum stressors. *Molecules*. 2018;23(2):337.
17. Hu K, Zatyka M, Astuti D, Beer N, Dias RP, Kulkarni A, Ainsworth J, Wright B, Majander A, Yu-Wai-Man P, et al. WFS1 protein expression correlates with clinical progression of optic atrophy in patients with Wolfram syndrome. *J Med Genet*. 2022;59(1):65–74.
18. Hofmann S, Philbrook C, Gerbitz KD, Bauer MF. Wolfram syndrome: structural and functional analyses of mutant and wild-type wolframin, the WFS1 gene product. *Hum Mol Genet*. 2003;12(16):2003–12.
19. Yamaguchi S, Ishihara H, Tamura A, Yamada T, Takahashi R, Takei D, Katagiri H, Oka Y. Endoplasmic reticulum stress and N-glycosylation modulate expression of WFS1 protein. *Biochem Biophys Res Commun*. 2004;325(1):250–6.
20. Osman AA, Saito M, Makepeace C, Permutt MA, Schlesinger P, Mueckler M. Wolframin expression induces novel ion channel activity in endoplasmic reticulum membranes and increases intracellular calcium. *J Biol Chem*. 2003;278(52):52755–62.
21. Mishra R, Chen BS, Richa P, Yu-Wai-Man P. Wolfram syndrome: new pathophysiological insights and therapeutic strategies. *Ther Adv Rare Dis*. 2021;2:26330040211039520.
22. Bucca BC, Klingensmith G, Bennett JL. Wolfram Syndrome: a rare optic neuropathy in youth with type 1 diabetes. *Optom Vis Sci*. 2011;88(11):E1383–1390.
23. Wang Y, Liu X, Xu Z. Endoplasmic reticulum stress in hearing loss. *J Otorhinolaryngol, Hear Balance Med*. 2018;1(1):3.
24. Bahar E, Kim JY, Yoon H. Chemotherapy resistance explained through endoplasmic reticulum stress-dependent signaling. *Cancers*. 2019;11(3):338.
25. Mehdizadehtapeh L, Obakan Yerllkaya P. Endoplasmic reticulum stress and oncomir-associated chemotherapeutic drug resistance mechanisms in breast cancer tumors. *Turk J Biol*. 2021;45(1):1–16.
26. Salaroglio IC, Panada E, Moiso E, Buondonno I, Provero P, Rubinstein M, Kopecka J, Riganti C. PERK induces resistance to cell death elicited by endoplasmic reticulum stress and chemotherapy. *Mol Cancer*. 2017;16(1):91.
27. Cagala M, Pavlikova L, Seres M, Kadlecikova K, Breier A, Sulova Z. Development of resistance to endoplasmic reticulum stress-inducing agents in mouse leukemic L1210 cells. *Molecules*. 2020;25(11):2517.
28. Seres M, Pavlikova L, Bohacova V, Kyca T, Borovska I, Lakatos B, Breier A, Sulova Z. Overexpression of GRP78/BiP in P-glycoprotein-positive L1210 cells is responsible for altered response of cells to tunicamycin as a stressor of the endoplasmic reticulum. *Cells*. 2020;9(4):890.
29. Polekova L, Barancik M, Mrazova T, Pirker R, Wallner J, Sulova Z, Breier A. Adaptation of mouse leukemia cells L1210 to vincristine. Evidence for expression of P-glycoprotein. *Neoplasma*. 1992;39(2):73–7.
30. Lorenz TC. Polymerase chain reaction: basic protocol plus troubleshooting and optimization strategies. *J Vis Exp*. 2012;63: e3998.
31. Nolan T, Hands RE, Bustin SA. Quantification of mRNA using real-time RT-PCR. *Nat Protoc*. 2006;1(3):1559–82.
32. Oslowski CM, Urano F. Measuring ER stress and the unfolded protein response using mammalian tissue culture system. *Methods Enzymol*. 2011;490:71–92.
33. Brunelle JL, Green R. One-dimensional SDS-polyacrylamide gel electrophoresis (1D SDS-PAGE). *Methods Enzymol*. 2014;541:151–9.
34. Bass JJ, Wilkinson DJ, Rankin D, Phillips BE, Szewczyk NJ, Smith K, Atherton PJ. An overview of technical considerations for Western blotting applications to physiological research. *Scand J Med Sci Sports*. 2017;27(1):4–25.
35. Schindelin J, Arganda-Carreras I, Frise E, Kaynig V, Longair M, Pietzsch T, Preibisch S, Rueden C, Saalfeld S, Schmid B, et al. Fiji: an open-source platform for biological-image analysis. *Nat Methods*. 2012;9(7):676–82.
36. Trieu EP, Gross JK, Targoff IN. Immunoprecipitation-western blot for proteins of low abundance. *Methods Mol Biol*. 2009;536:259–75.
37. Waterborg JH. The lowry method for protein quantitation. In: Walker JM, editor. *The protein protocols handbook*. Totowa, NJ: Humana Press; 2009. p. 7–10.
38. Sulova Z, Ditte P, Kurucova T, Polakova E, Rogozanova K, Gibalova L, Seres M, Skvarkova L, Sedlak J, Pastorek J, Breier A. The presence of P-glycoprotein in L1210 cells directly induces down-regulation of cell surface saccharide targets of concanavalin A. *Anticancer Res*. 2010;30(9):3661–8.
39. Sulova Z, Orlicky J, Fiala R, Dvoinova I, Uhrík B, Seres M, Gibalova L, Breier A. Expression of P-glycoprotein in L1210 cells is linked with rise in sensitivity to Ca²⁺. *Biochem Biophys Res Commun*. 2005;335(3):777–84.
40. Gene 22393. *NCBI gene database*, <https://www.ncbi.nlm.nih.gov/gene>. Accessed 3 Sep 2022.
41. De Falco M, Manente L, Lucariello A, Baldi G, Fiore P, Laforgia V, Baldi A, Iannaccone A, De Luca A. Localization and distribution of wolframin in human tissues. *Front Biosci*. 2012;4(5):1986–98.
42. Schmitz EA, Takahashi H, Karakas E. Structural basis for activation and gating of IP3 receptors. *Nat Commun*. 2022;13(1):1408.
43. Xu H, Van Remmen H. The sarcoendoplasmic reticulum calcium ATPase (SERCA) pump: a potential target for intervention in aging and skeletal muscle pathologies. *Skelet Muscle*. 2021;11(1):25.
44. Nogueira E, Cruz CF, Loureiro A, Nogueira P, Freitas J, Moreira A, Carmo AM, Gomes AC, Preto A, Cavaco-Paulo A. Assessment of liposome disruption to quantify drug delivery in vitro. *Biochim Biophys Acta*. 2016;1858(2):163–7.
45. Seres M, Polakova E, Krizanova O, Hudecova S, Klymenko SV, Breier A, Sulova Z. Overexpression of P-glycoprotein in L1210/VCR cells is associated with changes in several endoplasmic reticulum proteins that may be partially responsible for the lack of thapsigargin sensitivity. *Gen Physiol Biophys*. 2008;27(3):211–21.
46. Dunn KW, Kamocka MM, McDonald JH. A practical guide to evaluating colocalization in biological microscopy. *Am J Physiol Cell Physiol*. 2011;300(4):C723–742.
47. Wen T, Xue P, Ying J, Cheng S, Liu Y, Ruan D. The role of unfolded protein response in human intervertebral disc degeneration: perk and IRE1-alpha as two potential therapeutic targets. *Oxid Med Cell Longev*. 2021;2021:6492879.
48. Hsu SK, Chiu CC, Dahms HU, Chou CK, Cheng CM, Chang WT, Cheng KC, Wang HD, Lin IL. Unfolded protein response (UPR) in survival, dormancy, immunosuppression, metastasis, and treatments of cancer cells. *Int J Mol Sci*. 2019;20(10):2518.
49. Kopp MC, Larburu N, Durairaj V, Adams CJ, Ali MMU. UPR proteins IRE1 and PERK switch BiP from chaperone to ER stress sensor. *Nat Struct Mol Biol*. 2019;26(11):1053–62.
50. Turpin J, El-Safadi D, Lebeau G, Frumence E, Despres P, Viranaicken W, Krejbich-Trotot P. CHOP pro-apoptotic transcriptional program in response to er stress is hacked by zika virus. *Int J Mol Sci*. 2021;22(7):3750.
51. Park SM, Kang TI, So JS. Roles of XBP1s in transcriptional regulation of target genes. *Biomedicines*. 2021;9(7):791.
52. Wang H, Karnati S, Madhusudhan T. Regulation of the homeostatic unfolded protein response in diabetic nephropathy. *Pharmaceuticals*. 2022;15(4):401.
53. Li Y, Guo Y, Tang J, Jiang J, Chen Z. New insights into the roles of CHOP-induced apoptosis in ER stress. *Acta Biochim Biophys Sin*. 2014;46(8):629–40.
54. Takeda K, Inoue H, Tanizawa Y, Matsuzaki Y, Oba J, Watanabe Y, Shinoda K, Oka Y. WFS1 (Wolfram syndrome 1) gene product: predominant subcellular localization to endoplasmic reticulum in cultured cells and neuronal expression in rat brain. *Hum Mol Genet*. 2001;10(5):477–84.
55. Sulova Z, Seres M, Barancik M, Gibalova L, Uhrík B, Polekova L, Breier A. Does any relationship exist between P-glycoprotein-mediated multidrug

- resistance and intracellular calcium homeostasis. *Gen Physiol Biophys*. 2009;28:F89-95.
56. Seres M, Cholujska D, Bubencikova T, Breier A, Sulova Z. Tunicamycin depresses P-glycoprotein glycosylation without an effect on its membrane localization and drug efflux activity in L1210 cells. *Int J Mol Sci*. 2011;12(11):7772–84.
57. Pavlikova L, Seres M, Hano M, Bohacova V, Sevcikova I, Kyca T, Breier A, Sulova Z. L1210 cells overexpressing ABCB1 drug transporters are resistant to inhibitors of the N- and O-glycosylation of proteins. *Molecules*. 2017;22(7):1104.
58. Kurekova S, Plaas M, Cagalinec M. Lack of functional wolframin causes drop in plasmalemmal sodium-calcium exchanger type 1 expression at early stage in rat model of Wolfram syndrome. *Gen Physiol Biophys*. 2020;39(5):499–503.
59. Hu H, Tian M, Ding C, Yu S. The C/EBP homologous protein (CHOP) transcription factor functions in endoplasmic reticulum stress-induced apoptosis and microbial infection. *Front Immunol*. 2018;9:3083.
60. Yamaguchi H, Wang HG. CHOP is involved in endoplasmic reticulum stress-induced apoptosis by enhancing DR5 expression in human carcinoma cells. *J Biol Chem*. 2004;279(44):45495–502.
61. Yoshida H, Matsui T, Yamamoto A, Okada T, Mori K. XBP1 mRNA is induced by ATF6 and spliced by IRE1 in response to ER stress to produce a highly active transcription factor. *Cell*. 2001;107(7):881–91.
62. Fonseca SG, Ishigaki S, Oslowski CM, Lu S, Lipson KL, Ghosh R, Hayashi E, Ishihara H, Oka Y, Permutt MA, Urano F. Wolfram syndrome 1 gene negatively regulates ER stress signaling in rodent and human cells. *J Clin Invest*. 2010;120(3):744–55.
63. Gong Y, Xiong L, Li X, Su L, Xiao H. A novel mutation of WFS1 gene leading to increase ER stress and cell apoptosis is associated an autosomal dominant form of Wolfram syndrome type 1. *BMC Endocr Disord*. 2021;21(1):76.
64. Bubencikova T, Cholujska D, Messingerova L, Mislovicova D, Seres M, Breier A, Sulova Z. Detection of glycomic alterations induced by overexpression of p-glycoprotein on the surfaces of L1210 cells using sialic acid binding lectins. *Int J Mol Sci*. 2012;13(11):15177–92.
65. Pavlikova L, Seres M, Imrichova D, Hano M, Rusnak A, Zamorova M, Katrlík J, Breier A, Sulova Z. The expression of P-gp in leukemia cells is associated with cross-resistance to protein N-glycosylation inhibitor tunicamycin. *Gen Physiol Biophys*. 2016;35(4):497–510.
66. Sulova Z, Mislovicova D, Gibalova L, Vajcnerova Z, Polakova E, Uhrík B, Tylkova L, Kovarova A, Sedlak J, Breier A. Vincristine-induced overexpression of P-glycoprotein in L1210 cells is associated with remodeling of cell surface saccharides. *J Proteome Res*. 2009;8(2):513–20.
67. Lewy TG, Grabowski JM, Bloom ME. BiP: master regulator of the unfolded protein response and crucial factor in flavivirus biology. *Yale J Biol Med*. 2017;90(2):291–300.
68. Zatyka M, Da Silva XG, Bellomo EA, Leadbeater W, Astuti D, Smith J, Michelangeli F, Rutter GA, Barrett TG. Sarco(endo)plasmic reticulum ATPase is a molecular partner of Wolfram syndrome 1 protein, which negatively regulates its expression. *Hum Mol Genet*. 2015;24(3):814–27.
69. Gharanei S, Zatyka M, Astuti D, Fenton J, Sik A, Nagy Z, Barrett TG. Vacuolar-type H⁺-ATPase V1A subunit is a molecular partner of Wolfram syndrome 1 (WFS1) protein, which regulates its expression and stability. *Hum Mol Genet*. 2013;22(2):203–17.
70. Yurimoto S, Hatano N, Tsuchiya M, Kato K, Fujimoto T, Masaki T, Kobayashi R, Tokumitsu H. Identification and characterization of wolframin, the product of the wolfram syndrome gene (WFS1), as a novel calmodulin-binding protein. *Biochemistry*. 2009;48(18):3946–55.
71. Zatyka M, Ricketts C, da Silva XG, Minton J, Fenton S, Hofmann-Thiel S, Rutter GA, Barrett TG. Sodium-potassium ATPase 1 subunit is a molecular partner of Wolframin, an endoplasmic reticulum protein involved in ER stress. *Hum Mol Genet*. 2008;17(2):190–200.
72. Rozpedek-Kaminska W, Siwecka N, Wawrzynkiewicz A, Wojtczak R, Pytel D, Diehl JA, Majsterek I. The PERK-dependent molecular mechanisms as a novel therapeutic target for neurodegenerative diseases. *Int J Mol Sci*. 2020;21(6):2108.
73. Carew NT, Nelson AM, Liang Z, Smith SM, Milcarek C. Linking endoplasmic reticular stress and alternative splicing. *Int J Mol Sci*. 2018;19(12):3919.
74. Shen J, Snapp EL, Lippincott-Schwartz J, Prywes R. Stable binding of ATF6 to BiP in the endoplasmic reticulum stress response. *Mol Cell Biol*. 2005;25(3):921–32.

Publisher's Note

Springer Nature remains neutral with regard to jurisdictional claims in published maps and institutional affiliations.